A progressive collapse modelling strategy coupling the yield design theory with non-linear analysis

Mohammad EL HAJJ DIAB[1], André ORCESI [2*], Cédric DESPREZ[3] and Jérémy BLEYER[4]

ABSTRACT: Several examples of structures have been severely damaged, or even reached the total collapse, after the propagation of some local failure, resulting from an accidental or exceptional event. These catastrophic events highlight the importance of not limiting safety assessment in structural design under identified conditions, but also to investigate how much the structural integrity can be preserved so that progressive collapse is avoided under an exceptional event unidentified at the design stage.

The main objective of this work is to propose a progressive collapse modelling approach in order to characterize structural robustness. Considering the occurrence of some exceptional event, the yield design theory is used to identify the part of the structure concerned by a failure mechanism. As the yield design theory is based on the infinitesimal strain assumption, an iterative coupling between the yield design approach and a non-linear analysis of the directly affected part is proposed to (i) better analyze the structural response of the part concerned by the failure mechanism, (ii) consider the development of materials and geometrical non-linearities, and (iii) model progressive collapse within the structure. The successive iterations of the yield design approach including the deformed geometrical configuration allow to check the potential ability of the structure to develop a second line of defence. This coupling strategy is applied to a steel framed structure for illustration of the proposed concepts.

[1] MAST-EMGCU, Univ Gustave Eiffel, IFSTTAR, F-77447 Marne-la-Vallée, France
[2] * MAST-EMGCU, Univ Gustave Eiffel, IFSTTAR, F-77447 Marne-la-Vallée, France, corresponding author : E-mail : andre.orcesi@univ-eiffel.fr
[3] MAST-EMGCU, Univ Gustave Eiffel, IFSTTAR, F-77447 Marne-la-Vallée, France
[4] Laboratoire Navier, ENPC, Univ Gustave Eiffel, CNRS, F-77447 Marne-la-Vallée, France

Keywords: Structural robustness, progressive collapse, disproportionate collapse, local failure, yield design approach, nonlinear analysis.

1. INTRODUCTION

The world has witnessed many incidents of progressive collapses on various types of structure (bridges, airports, towers, etc.), under several types of triggering events (natural hazard, blast, impact, construction errors, etc.). The associated consequences, whether human, economic or environmental, have often put robustness issues on the table (Faber et al., 2006, Baker et al., 2008, COST Action TU0601, 2011, Kagho-Gouadjio et al. 2015, Hoffmann et al. 2015, Demonceau et al. 2018) and pushed the civil engineering community to further analyze structural behaviour under abnormal actions.

After the Second World War, Baker et al. (Baker et al.,1948) studied the behaviour of structures against bomb explosions and debris impacts in London during the war and identified progressive collapse in several cases of structural failures. The partial and progressive collapse of the Ronan Point Tower, in London on 16 May 1968 is one of the most famous historical failures, where an internal gas explosion on the 18th floor dislodged one of the exterior walls, which propagated and led to the collapse of the entire corner of the building (Pearson and Delatte, 2005). This collapse was a decisive moment when structural robustness began to gain importance. As the consequences were considered unacceptable to the initial damage, some regulations for design against disproportionate collapse were introduced in the British design code "The Building (fifth Amendment) Regulations 1970". In 2001 the collapse of the World Trade Centre (WTC) Twin Towers, due to the impact of large commercial aircraft in New York City (NIST, 2006), led to a significant interest in the structural robustness issue. The research effort intensified in parallel of the development of structural design codes that introduce novel instructions and provisions (Demonceau 2008, Droogné et al. 2018, Adam et al., 2018). Many other collapses also highlight the issue of structural robustness, such as the partial collapse of

Terminal 2E at Charles-de-Gaulle Airport in France in 2004 (El Kamari et al., 2015), the collapse of the I-35W Bridge in the USA in 2007 (NTSB, 2008), the collapse of the Genoa Bridge in Italy in August 2018, and of Nanfang'ao Bridge in Taiwan in October 2019. For each of these examples, a local failure led to an extended collapse.

During its service life, a structure might not be able to resist some of the actions not considered at the design stage, or for example in case of advanced degradation of structural components. An event might lead to a local failure with a partial collapse of some structural elements that can propagate and cause the failure of other components in the structure (Nafday et al. 2011). The spread of failure propagation not only depends on the magnitude of the local failure, but also on the capacity of the structure to prevent or to mitigate this propagation.

Progressive collapse analysis represents an essential tool in the structural robustness assessment. The features needed for progressive collapse modelling are related to the identification of the main aspects in the approach of the structural robustness quantification. These features are described as below:

- to perform an overall assessment of structural robustness, a large number of scenarios have to be considered. Therefore, a simplified structural modelling method is required to model the structural response under the applied scenario with a reasonable computation time;
- to assess the degree of failure propagation, the initial and the final states of failure have to be identified. Thus, the structural modelling method should follow the propagation of failure, starting from the initial failure until the final stage of failure, including the successive loss of structural elements.
- With the view to achieve a simulation of progressive collapse close to reality, the essential aspects of progressive collapse analysis have to be taken into account, which

relate to the geometrical and materials non-linearities as well as the dynamic effects due to the loss of structural elements.

There are different levels of discretization for structural modelling of progressive collapse (local, global, and semi-global), where the choice depends on the dimensions of the structure and the level of precision required (Ulm, 1996). The local approach accurately simulates the structural response, using proper material constitutive modelling but at a significant computational cost, especially when dealing with non-linearities or numerous scenarios. Its application to exceptional situations can be found in Bao et al. (2008), Sadek et al. (2011), and Gao et al. (2017). In a global approach, the structure is modelled with beam/shell elements, and a global constitutive law expressed in terms of force resultants. Significant computation time savings can be obtained at the expanse of less detailed representation of local material behaviour, especially in case of heterogeneous sections (reinforced concrete, damage, etc.). The global approach has been used to simulate an entire building in three-dimensional (3D) with nonlinear dynamic analysis (Fu, 2010; Li et al., 2011; Song and Sezen, 2013). An intermediate scale of discretization is presented by the semi-global approach, where the element section can be discretized using multi-layer or multi-fiber elements, each layer or fiber having its own constitutive law (Mazars and Grange, 2017). It has been widely used in the progressive collapse analysis, whether under threat-dependent scenarios (Sun et al., 2012; Lu et al., 2017), or threat-independent scenarios (Bao et al., 2014; Kazemi-Moghaddam and Sasani, 2015; Li et al., 2016). Furthermore, Tagel-Din and Meguro (2000) developed the Applied Element Method to model the entire collapse process which consists in an assembly of small rigid elements, connected together by sets of normal and shear springs. This method can simulate the structure progressive collapse, starting from crack initiation and propagation, element separation, formation of debris and collision between falling debris and other structural components in reasonable time. It has been used in recent years to simulate the progressive collapse of structures as Sasani (2008) and

Marginean et al. (2018). Moreover, in the context of applying the Alternative load paths method, an analytical approach was developed at the University of Liège that allows predicting the response of building frames submitted to a column loss, and in particular, the associated catenary actions (Demonceau, 2008; Jaspart et al., 2011; Demonceau et al., 2018).

The non-linear dynamic analysis allows to simulate the structural response by taking into account non-linearities and dynamic effects. Therefore, it is the most accurate method to simulate the progressive collapse (DCLG and CPNI, 2011; Stylianidis, 2011). However, the non-linear dynamic analysis is often very time-consuming and vulnerable to non-convergence issues. Hence, a non-linear static analysis is commonly used for the progressive collapse simulation. Furthermore, many studies and international codes propose to consider the dynamic effects by amplifying the gravity loading with a dynamic amplification factor (EN 1990, 2003; UFC 4-023-03, 2009; Marchand and Alfawakhiri, 2005). Besides, Izzuddin et al. (2008) propose an energy-based approach to define the pseudo-static response of building structures subject to sudden column loss.

In this work, one aims to provide a framework for progressive collapse modelling. The key question addressed here is how to propose a simplified modelling of progressive collapse by considering the dynamic effects due to some element loss, the geometrical and the material non-linearities. For structural robustness assessment purposes, there is a high uncertainty level associated with the type and intensity of exceptional actions, so a large number of scenarios should be investigated and the structural modelling should effectively describe failure propagation.

To address these questions, the proposed method takes advantage of coupling the yield design and the non-linear finite element modelling strategies.

On the one hand, the yield design approach is used to detect the successive failure mechanisms that could occur in the structure. This direct method enables to determine the ultimate load of a

structure, thus avoiding a step-by-step non-linear analysis of the structural response along the full loading path until failure (De Buhan, 2007a). On the other hand, the non-linear analysis is restricted to the sub-structure directly affected to compute structural evolution in non-linear domain. This coupling strategy is an iterative procedure to check if an alternative load path can be found in the area close to the directly affected part of a structure, and if not, how the failure propagation can be discretized until one reaches a final stage.

The paper is organized as follows. The key points of the yield design theory are reminded in Section 2, with the presentation of the static and the kinematic approaches. Then, the coupling between yield design and non-linear analyses is described in Section 3 and the numerical modelling of both approaches used for progressive collapse analysis is introduced in Section 4. Finally, this coupling strategy is applied in Section 5 to a steel framed case study for illustration.

2. YIELD DESIGN APPROACH BACKGROUND

The theory of yield design (or limit analysis in the context of perfectly plastic materials) is based upon the analysis of the conditions ensuring the compatibility between the equilibrium of the structure and the local verification of a strength criterion at any point of the structure (Salençon, 2013). This method consists of the application of two approaches, static and kinematic, that enable to approximate and bracket the ultimate load of the structure by lower and upper bounds, respectively. The main benefit of this method is its ability to investigate the ultimate state of the structure with avoiding complex non-linear computations with potential convergence issues, and significantly saving computational costs. Besides, this method provides valuable information such as the failure mechanism and the most critical areas of the structure. Principles of the yield design theory can be explicitly found in the strut-and-tie modelling (NF EN 1992-1-1, 2005). Strut-and-tie models consist of struts representing compressive stress fields, of ties representing the reinforcement, and of the connecting nodes. The forces in the elements of a strut-and-tie model should be determined by maintaining the

equilibrium with the applied loads in the ultimate limit state. In some way, this approach can be related to the lower bound static approach of yield design (Vincent et al., 2017).

The yield design approach is based upon the infinitesimal strain theory, meaning that the geometrical deformation is neglected. The important concepts are now recalled for a 3D continuum Ω. The applied loading mode is defined through $\underline{Q}$ $(Q_i, i = 1, \dots, n)$ depending on n parameters. The loading can be body forces (gravity for example) or surface forces on the edge of the structure. The constituent material strength properties are characterized, at each point $\underline{x}$ of the system Ω, by a convex strength domain $G(\underline{x})$. Therefore, an admissible stress tensor $\underline{\underline{\sigma}}(\underline{x})$ has to comply with the following strength condition:

$$\forall \underline{x} \in \Omega, \underline{\underline{\sigma}}(\underline{x}) \in G(\underline{x}) \tag{1}$$

The yield design approach enables to identify the domain of potentially safe loads K based on the compatibility between the equilibrium of the structure and the local resistance at any point of the structure. The domain of potential safe loads K is defined as the set of loads $\underline{Q}$, for which there exists a stress tensor $\underline{\underline{\sigma}}(\underline{x})$ statically admissible with the loading mode $\underline{Q}$ and for which the strength condition is satisfied at each point of the system i.e.:

$$\underline{Q} \in K \iff \begin{cases} 1.\ \exists\, \underline{\underline{\sigma}}(\underline{x}) \text{ statically admissible in the loading mode with load } \underline{Q} & \text{(equilibrium condition)} \\ 2.\ \underline{\underline{\sigma}}(\underline{x}) \in G(\underline{x}), \forall\ \underline{x} \in \Omega & \text{(resistance condition)} \end{cases} \tag{2}$$

Restricting the above definition to a finite set of statically admissible stress fields, a lower bound estimate of the potentially safe loads domain can be obtained.

Let us also mention that yield design (or limit analysis) theory offers an alternative characterization of the domain of potentially safe loads through the so-called kinematic approach. Relying on the use of virtual collapse mechanisms, equilibrium equations are written in a weak fashion using the virtual work principle. The structure stability is ensured if and only

if the work of external forces is less than the maximum resisting work, see more details in (de Buhan, 2007b; Salençon, 2013). Applying the kinematic approach on a finite set of potential collapse mechanisms, obtained through a finite-element discretization for instance, yields an upper bound estimate to the structure collapse load.

The yield design approach enables to approximate and bracket the ultimate load Q_u of the structure by a lower bound $Q_{u,s}$ with the static approach and upper bound $Q_{u,k}$ with the kinematic approach ($Q_{u,s} < Q_u < Q_{u,k}$), and it also identifies the corresponding failure mechanism. One can then identify the capacity of the structure and estimate if the structure can resist a load Q under an exceptional situation. The structure is assumed to be able to resist an applied load if $Q < Q_{u,s}$, which indicates that the structure can support the applied load without any failure. Conversely, the structure is unable to resist an applied load if $Q > Q_{u,k}$, meaning that the structure fails under the mechanism identified by the kinematic approach of yield design. By comparing the applied load Q with $Q_{u,s}$, which is the lower bound of the ultimate load estimation, one avoids the overestimation of the structural capacity.

The corresponding failure mechanism identifies the directly affected part, and the critical points of the structure in which the structural element cannot resist the applied forces. Besides, the failure mechanism also allows to estimate if there is either a loss of stability of the directly affected part, or the possibility to develop an alternative functioning. When the failure mechanism indicates the mechanical instability of some elements under the applied load, there is no interest to simulate the geometrical displacements of the affected part after the failure. Conversely, if the failure mechanism reveals a potential alternative equilibrium state, the geometrical displacements might lead to a change in the redistribution of the forces in the elements, and the structure might be able to function in a different manner. Furthermore, this alternative functioning can increase the structural capacity to withstand the applied load. Therefore, there is an interest to simulate the geometrical changes in this case, and to study the

evolution of the structural capacity with the geometrical displacements in order to investigate the change in ability of the structure to resist the applied load. As the yield design approach is based on infinitesimal strain assumption, considering that the materials are elastic perfectly plastic, the main challenge to use this method for robustness analysis is to consider the geometrical non-linearities and to iteratively simulate the propagation of the failure. Using a non-linear analysis on the affected part identified by the yield design is proposed thereafter to offset the limits of the yield design calculation.

3. COUPLING BETWEEN THE YIELD DESIGN APPROACH AND A NON-LINEAR ANALYSIS

The principle of coupling a yield design approach with another type of analysis was used by Pham (2014) and Bleyer (2015) to model the geometrical and material changes. The behaviour of a reinforced concrete panel under the fire action was considered and a thermo-elastic analysis was used to identify the geometrical displacements. The materials degradation was then integrated in a yield design calculation in order to identify the stability factor of the deformed structure.

This study proposes an embedded yield design approach within a non-linear analysis. In order to follow the propagation of failure and identify the successive structural states, an iterative procedure of yield design calculation is proposed (El Hajj Diab et al., 2019, El Hajj Diab, 2019). At each step i of the iterative process, the yield design calculation checks the ability of the structure to resist the applied load Q, and identifies the failure mechanism if $Q > Q_{u,s}^{i}$. The proposed structural modelling strategy is based on the coupling between the yield design approach and the non-linear analysis in an iterative procedure. This procedure is illustrated in Figure 1, with the following steps (each step is identified in Figure 1):

1) The yield design approach is applied to identify the ultimate load $Q_{u,s}$ and the failure mechanism.

2) $Q_{u,s}$ and applied loads Q are compared.

3) If $Q < Q_{u,s}$, the current structural configuration can support the applied load, and the failure stops at this stage.

4) If $Q \geq Q_{u,s}$, a failure mode potentially occurs under the applied loads.

5) The failure mechanism identified by the kinematic approach allows to identify the affected part and to estimate if there is either a loss of stability or the possibility to develop an alternative functioning.

6) The possibility of developing an alternative functioning by the tensile membrane action is investigated by checking whether the joints on both sides of the directly affected part (Figure 2a) are connected to the indirectly affected part or not.

7) If there is no continuity of the directly affected part beams with the indirectly affected parts on both sides, the failure mechanism indicates a mechanical instability of some elements, and the affected part is removed for the next iteration of the yield design calculation. If the entire structure is affected, then the overall structure collapses.

8) If the failure mechanism reveals that the directly affected part may develop an alternative functioning after large displacement, a non-linear analysis is applied to this part, in order to calculate the geometric displacements. The effect of the indirectly affected part on the substructure of the directly affected part is taken into account by considering horizontal springs at the extremities N_i of the substructure, as shown in Figure 2b. The rotation and the vertical displacement are restrained at N_i with allowing the horizontal displacement, and the springs are attached to fixed supports. In order to characterize these springs, the indirectly affected part is assumed to be perfectly elastic as assumed in

Demonceau (2008), and the springs are assumed as fully elastic. The stiffness K_i of each spring is calculated by applying a unitary force ($1kN$) at the i^{th} corresponding extremity (Figure 2c), where K_i is described as follow:

$$K_i = \frac{1}{u_{N_i}} \tag{3}$$

where u_i is the horizontal displacement of the joint N_i.

9) A non-linear analysis is applied on the substructure identified in the previous step with a view to identify the geometrical change under the applied loads Q.

10) The geometric changes are integrated in the next iteration of the yield design calculation by updating the structure geometry.

11) The iterative procedure continues until the end of collapse, for which the ultimate load on remaining elements is larger than the applied load, or until total collapse of the structure.

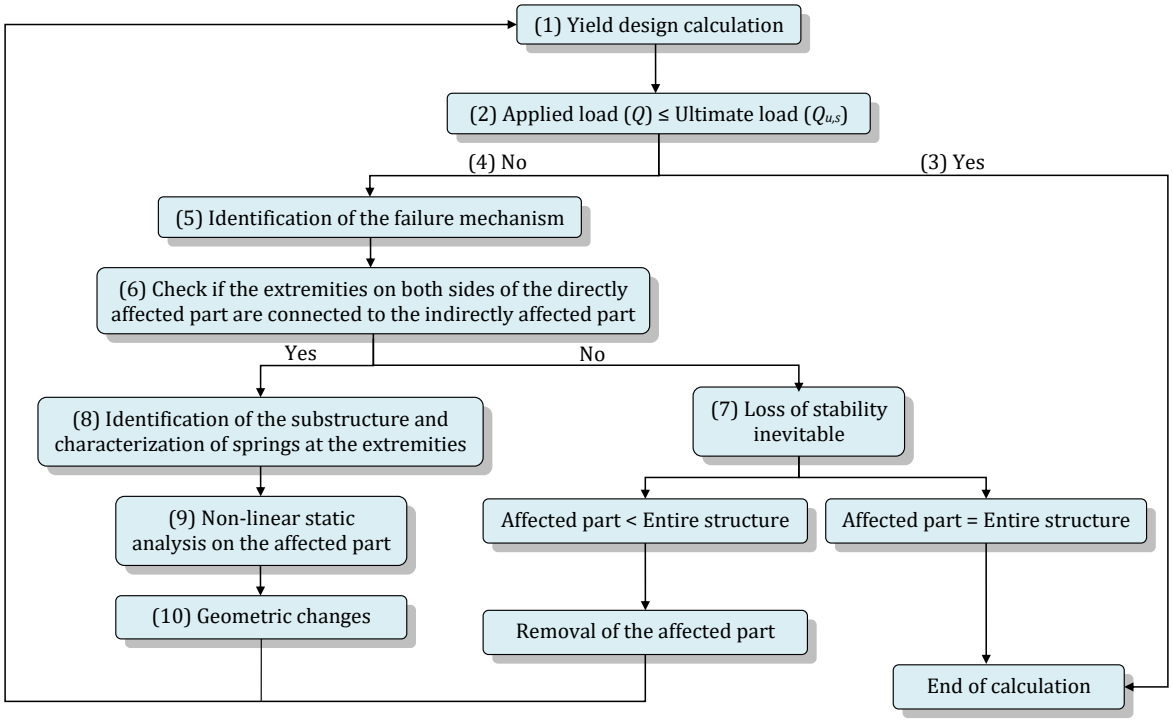

Figure 1. Proposed structural modelling strategy for progressive collapse analysis.

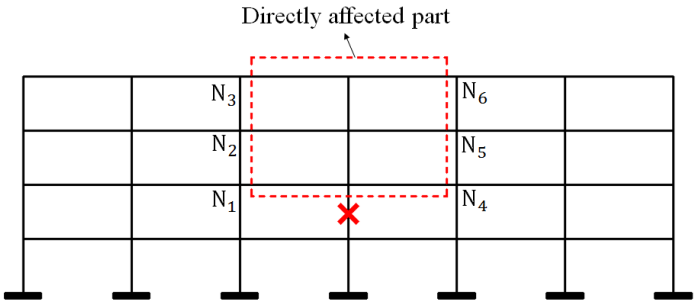

(a) Column loss scenario

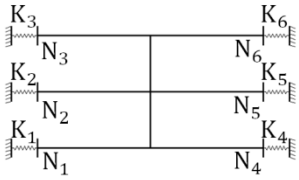

(b) Substructure of the directly affected part

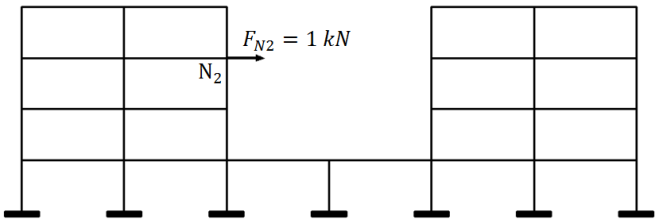

(c) Applied load to identify the spring stiffness on the joint N_2

Figure 2. Characterization of springs of the substructure.

In order to take into account the dynamic effects resulting from a geometrical modification after the loss structural component, though preventing the use of a full dynamic analysis, the structural response can be estimated from a non-linear static response under amplified gravity loading using a dynamic amplification factor. This aspect is mentioned in many codes and standards, such as EN 1990 (2003), GSA (2003), and UFC 4-023-03 (2009). The recommended value of the dynamic amplification factor is often 2.0, and the load amplification should only be applied over the bays adjacent to the removed elements. Otherwise, Marchand and Alfawakhiri (2005) mentioned that the factor of 2.0 is very conservative, and that a value between 1.3 and 1.5 is more realistic for a non-linear analysis when members achieve significant plastic rotation and displacements.

The idea of the proposed approach is to discretize the failure propagation associated with progressive collapse and to exploit the benefits of yield design approach in the progressive collapse simulation. The principal advantage is to identify the ultimate load and the failure

mechanism in a direct manner, then avoiding some convergence issues, and significantly saving computational costs. The role of the iteration of the yield design calculation is to identify whether or not there is a failure under the applied load. Furthermore, the identification of the failure mechanism allows to identify the directly affected part and then to identify whether or not there is a need to apply a detailed analysis with a non-linear analysis. Hence, the importance of the proposed method is to avoid the detailed analysis in the cases where there is no need, and to apply the detailed analysis on a localised part of the structure.

4. PROGRESSIVE COLLAPSE ANALYSIS FOR FRAMED STRUCTURES

4.1. Numerical modelling of yield design approach

The model proposed by Bleyer and de Buhan (2013) is used herein to approximate the ultimate load by some lower and upper bounds for frame structures. The static approach requires the maximization of a variable parameter with solving a linear optimization problem under non-linear convex constraints. Conversely, the kinematic approach requires the minimization of a variable parameter with solving a non-linear convex optimization problem under linear constraints. The model considers that the element is infinitely resistant with respect to shear and torsion forces. The yield criterion G_u is identified in the 3D space involving axial force N and the bending moments M_y and M_z based on an analysis of the cross-section material properties.

To check the local resistance of structural components in a global structure, Bleyer and de Buhan (2013) proposed an approximation procedure to describe the yield surface with a few parameters only.

In addition to strength limits based on the cross-section material properties, critical buckling loads are also verified according to Euler load formulation (NF EN 1992-1-1, 2005), which is expressed as:

$$N_{Euler} = \frac{\pi^2 E I_{min}}{l_f^2} \tag{4}$$

where EI_{min} is the minimum bending stiffness, and l_f is the effective length of the beam element. The boundary conditions of the element are considered as fixed for the numerical mockup of the following case study. Hence, $l_f = 0.5l$, where l is the element length. It is worth to note that the Euler formula represents the capacity of a perfectly elastic column to resist flexural buckling under compression, as a function of its elastic stiffness (EI) and interaction with yielding (Zhao et al., 2005). This equation is considered in the following as a first approximation and further detailed interaction relationship between axial compression and bending should be used in future studies for beam-column elements.

The ultimate load computation, from either a static or a kinematic approach and after a finite-element discretization, finally consists in solving a second-order cone programming (SOCP) problem, for which very efficient interior-point solvers are available, such as Mosek (Mosek, 2010) for instance. More detailed information can be found in the article of Bleyer and de Buhan (2013).

4.2. Numerical modelling of non-linear analysis

The MATLAB toolbox FEDEASLab (Filippou and Constantinides, 2004) is used to apply the non-linear static analysis, where the multilayer approach is applied in the structural modelling. The choice of this approach is based on (i) the possibility to consider the geometrical and material non-linearities with providing local information about the state of section and materials, and (ii) the computation cost of this method which is lower than with a local approach regarding the need for multi-scenario analysis. FEDEASLab enables to study the response of a 2D beam element with distributed inelasticity under non-linear geometry (Spacone et al., 1996). The non-linear analysis is performed by using the imposed displacement method, where the displacement increment enables to control structural behaviour close to the collapse and prevent

the frame from drifting apart suddenly in the ultimate state (Nutal, 2014). The corotational formulation (Le et al., 2011; Le, 2013; Le et al., 2014) is chosen to take into account the geometrical non-linearities using the FEDEASLab toolbox that integrates the effect of the large displacements and rotations). It should be mentioned that the shear effects are neglected herein when modelling the directly affected part, which is accepted herein for medium to large span to depth ratios of the member. For the examples considered in the following, the constitutive law of materials in the non-linear analysis is assumed as a bilinear elastic, perfectly plastic relationship. Such assumption is considered in the non-linear analysis with a view to be compatible with the yield design calculation.

5. APPLICATION TO A STEEL-FRAMED STRUCTURE

The structure considered for illustration is a 2D representative five-storey steel-framed building with ten bays. The geometric layout of the numerical mockup is presented in Figure 3. The bay dimensions are $6m$ or $5m$ in the *x* direction and $4m$ in the *y* direction. The constitutive structural elements are beams with cross-section IPE360, and columns with cross-section HEB500. Material properties are those of S355 steel grade, where the yield limits is 355 MPa and the elastic Young Modulus (E) is 210 GPa. The floors consist of 25 cm thick reinforced concrete slabs carried by the principal steel beams. The beam/column and column/footing connections are considered as rigid joints as no additional bracing is used.

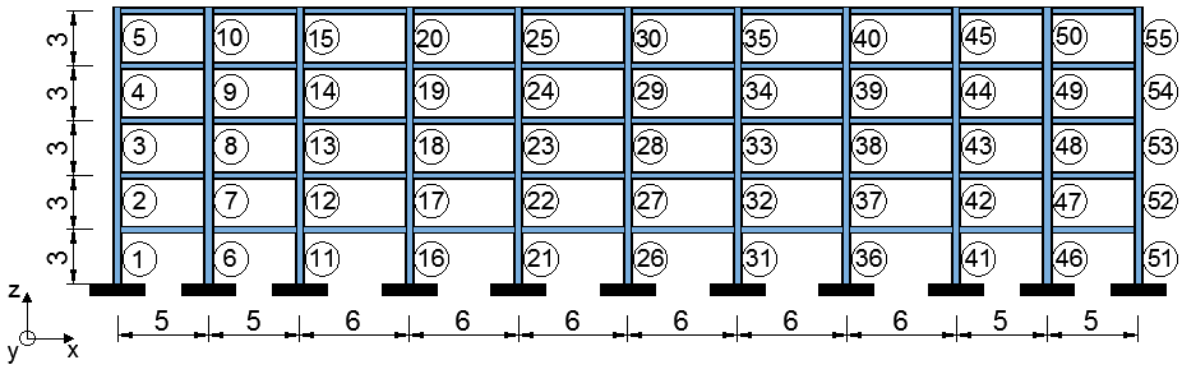

Figure 3. Layout of steel-frame building (dimensions in meter).

The constitutive elements are meshed with beam elements of length 0.25 m, so the columns are discretized into 12 elements and the beams are discretized into 24 or 20 elements according to the span length. The model was meshed using 1780 Bernoulli 2D Beam Finite Elements with Gauss-Lobatto integration points with 3 degrees of freedom per node.

The yield surfaces of the constitutive elements are calculated according to the model of Bleyer and de Buhan (2013) for both, IPE360 beams and HEB500 columns profiles. The cross-section was discretized using 164 triangular finite elements and material properties are those of S355 steel grade. The yield surfaces of beams and columns cross-section are presented in Figures 4 and 5, respectively. For better graphical representation, the yield surface is presented in the non-dimensional space (n, m_y, m_z) defined below:

$$\begin{cases} n & \frac{N}{N_0}; \quad N_0 = \frac{|min(N)| + |max(N)|}{2} \\ m_y & \frac{M_y}{M_{y0}}; \quad M_{y0} = \frac{|min(M_y)| + |max(M_y)|}{2} \\ m_z & \frac{M_z}{M_{z0}}; \quad M_{z0} = \frac{|min(M_z)| + |max(M_z)|}{2} \end{cases} \tag{5}$$

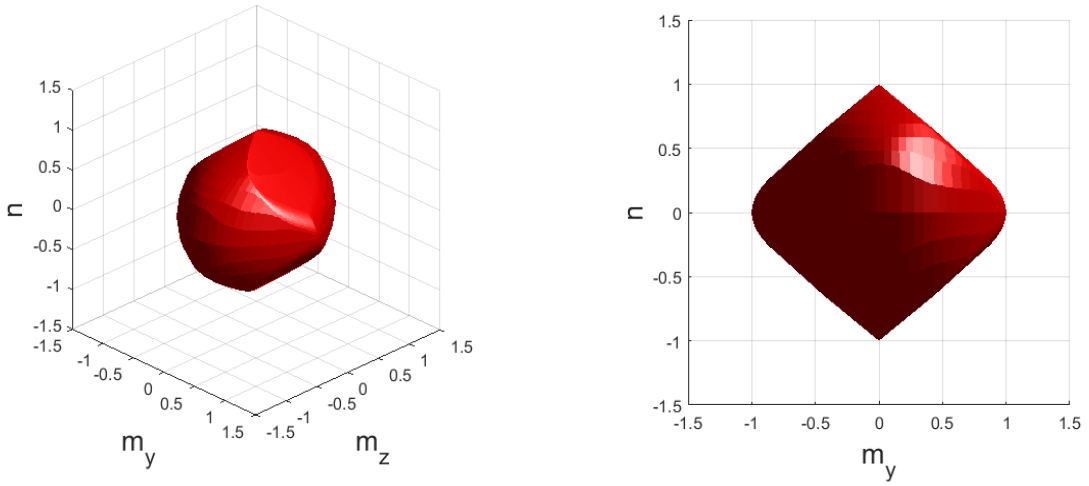

(a) View in (n, m_y, m_z) (n, m_y, m_z)non-dimensional space

(b) View in (n, m_y) (n, m_y) non-dimensional space

$N = n * N_0$; N_0= 8,250.0 kN
$M_y = m_y * M_{y0}$; M_{y0}= 1,662.0 kN.m
$M_z = m_z * M_{z0}$; M_{z0}= 474.0 kN.m

Figure 4. Yield surface of HEB500 steel column cross-section.

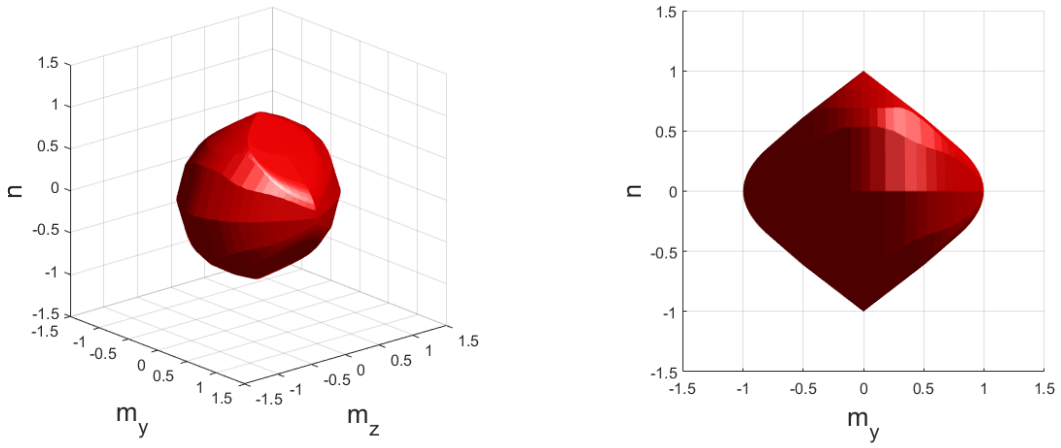

(a) View in (n, m_y, m_z) non-dimensional space (b) View in (n, m_y) non-dimensional space

$$N = n * N_0; N_0 = 2{,}483.0\ kN$$
$$M_y = m_y * M_{y0}; M_{y0} = 346.0\ kN.m$$
$$M_z = m_z * M_{z0}; M_{z0} = 76.3\ kN.m$$

Figure 5. Yield surface of IPE360 steel beam cross-section.

The local failure scenarios adopted in this example are limited to the notional total loss of one or several adjacent column(s), which is assumed to represent the occurrence of a local exceptional event. Dead loads include steel frame components and concrete slabs with a respective density of $78{,}50\ kN/m^3$, and $25 kN/m^3$. Besides, the live loads on floors are equal to $3\ kN/m^2$ according to the Eurocodes NF EN 1991-1-1 (2003), where the structure is considered as an administration building. The beams are then subject to uniform loads, where the values of dead loads (DL) and live loads (LL) are $25.6\ kN/m$ and $12\ kN/m$, respectively. The combination of actions DL and LL refers to an ultimate state as recommended in the Eurocodes NF EN 1990 (2003) for an accidental situation, for which one can mitigate the reserve on the applied loads by using smaller partial factors than those with a persistent situation, as follows:

- persistent situation: $W_p = 1.35DL + 1.5LL$
- accidental situation: $W_a = DL + 0.5LL$ (6)

This design configuration respects the Eurocodes serviceability and ultimate limit states. Moreover, the load capacity of the intact structure is verified under the combination of loads in the persistent situation $W_p = 52.5\ kN/m$. In the structural robustness assessment, the

combination of loads used under the local failure scenarios corresponds to the accidental situation $W_a = 31.6\,kN/m$. Further, the dynamic amplification factor used in this example is 1.5. The load amplification is applied only on the directly affected part, which normally contains all the beams, columns and beam-to-column joints located just above lost column(s). The structural response under the applied local failure scenarios can be classified into four categories, as described below:

- C1 without consequences: the local failure does not lead to any failure mechanism,

- C2 without collapse of the directly affected part: a failure mechanism is initiated according to the yield design theory. For a frame structure, the directly damaged part contains beams, columns and beam-to-column joints located just above lost column(s). However, the structure succeeds to find a second line of defence (i.e. by the catenary action developed in the directly affected part),

- C3 with collapse of the directly affected part: the structure does not succeed to find a second line of defence, and the failure mechanism leads to a partial collapse without further propagation beyond the first failure mechanism,

- C4 expanded collapse: the indirectly affected part of the structure cannot support the redistribution of loads in the new structural configuration and the collapse propagates out of the directly affected part.

The affected or the collapsed parts are quantified by the length of associated beams, where this value represents the consequences and the part of a structure that becomes out of service. The ultimate loads identified by the yield design calculation are noted as $Q_{u,s}^{Ci,j}$ and $Q_{u,k}^{Ci,j}$ for static

and kinematic approaches, respectively, where i represents the category of the local failure scenario Ci, and j is the iteration number of yield design calculation.

5.1. Illustration of local failure scenario C1

The first scenario of local failure is the notional loss of column # 6. Figure 6 shows the loading mode of the structure under this local failure scenario, and it shows the amplification of load on the directly affected part by the factor 1.5 to represent the dynamic effect. The first iteration of the yield design calculation indicates that $Q_{u,s}^{C1,1} = 37.7\,kN/m$ and $Q_{u,k}^{C1,1} = 39.2\,kN/m$. As $W_a(31.6\,kN/m) < Q_{u,s}^{C1,1}(36.7\,kN/m)$, the structure can resist the loss of the column # 6 without initiation of any failure mechanism (category C1).

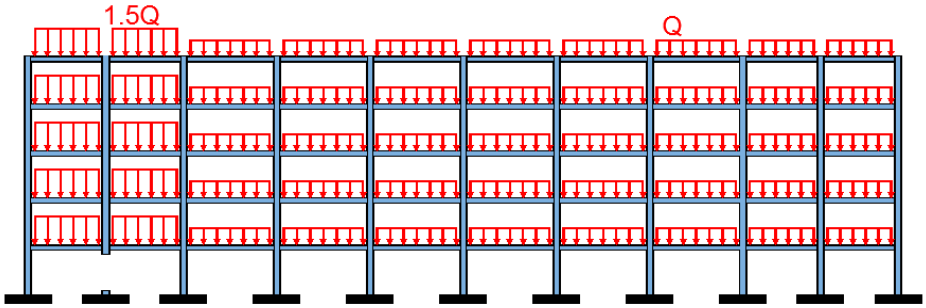

Figure 6. Notional loss of column # 6.

The non-linear static analysis on the whole structure indicates that the ultimate load is $Q_{u,NL}^{C1} = 38.8\,kN/m$ (Figure 7), where $Q_{u,s}^{C1,1} < Q_{u,NL}^{C1} < Q_{u,k}^{C1,1}$. The computation cost with the non-linear static analysis is $t_{C1}^{NL} = 1{,}230.0s$, while it can decrease by using the proposed coupling strategy to $t_{C1}^{CS} = 14s$ with one iteration of yield design calculation.

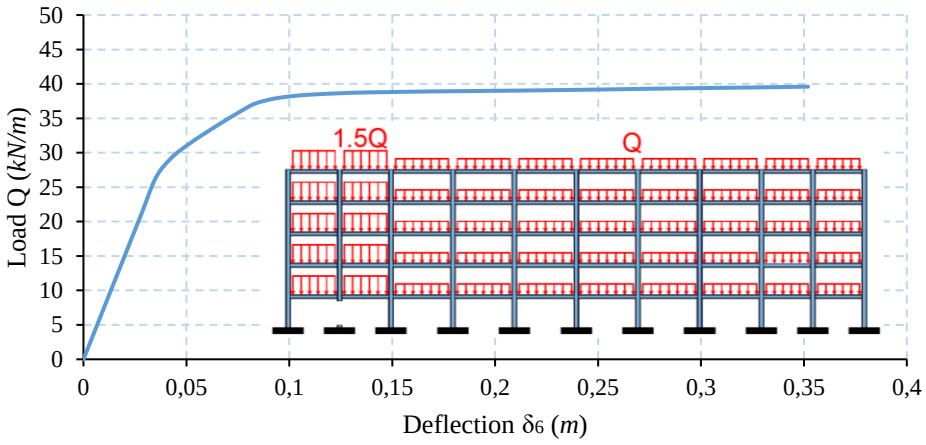

Figure 7. Deflection δ_6-load diagram of non-linear static analysis on the whole structure after the loss of column # 6.

5.2. Illustration of local failure scenario C2

The second scenario is the notional loss of column # 26, as shown in Figure 8 with the loading mode of the structure. The first iteration of the yield design calculation indicates that $Q_{u,s}^{C2,1} = 23.8\,kN/m$ and $Q_{u,k}^{C2,1} = 25.1\,kN/m$. As $Q_{u,s}^{C2,1} < W_a = 31.6\,kN/m$, the structure cannot resist the applied load W_a in initial geometry and a plastic mechanism occurs. The failure mechanism shown in Figure 9 indicates the possibility of developing an alternative functioning, where the continuity of the beams in both sides of the affected part allows the development of tensile membrane action in large displacement range. Therefore, a non-linear analysis is performed on the affected part to identify the geometric changes under the amplified loads ($1.5W_a$). The damaged area of the first iteration is considered as the initial damaged part (IDP), which is equal to $60m$ in this case (sum of beam length in this part of the structure). This indicator allows to evaluate the size of the part directly affected after the initial local failure.

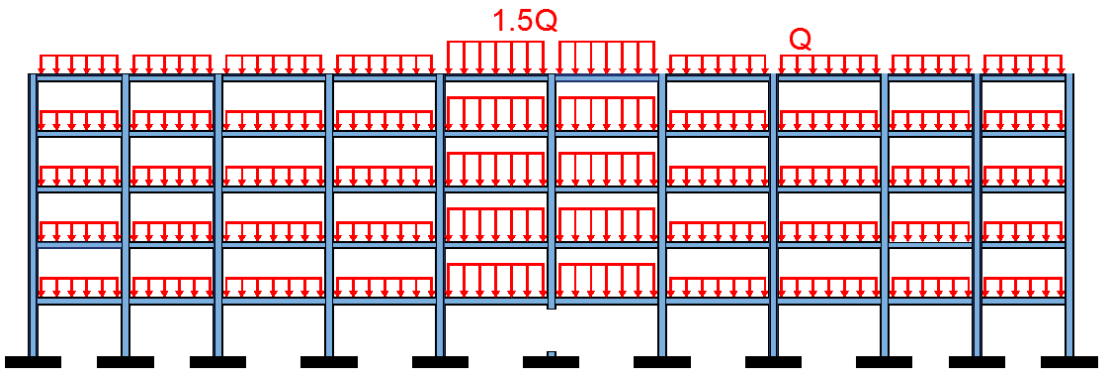

Figure 8. Notional loss of column # 26.

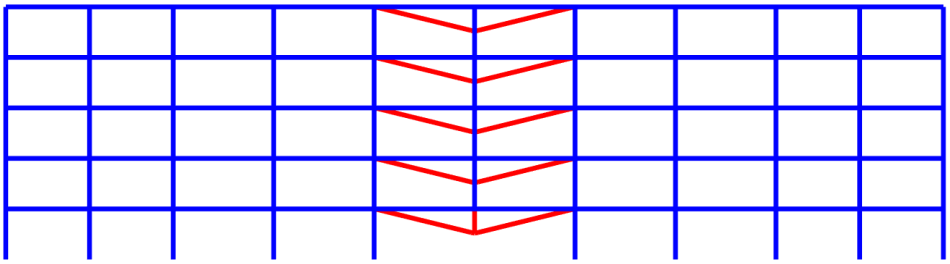

Figure 9. Failure mechanism identified by the first iteration of the yield design calculation after the loss of column # 26.

The substructure corresponding to the initial damaged part is presented in Figure 10. The stiffness of the spring at each extremity of the substructure is identified according to Equation (3). As the indirectly affected part is symmetric for both sides of the directly affected part, the stiffness of springs are similar for both sides of each story, as shown in Table 1.

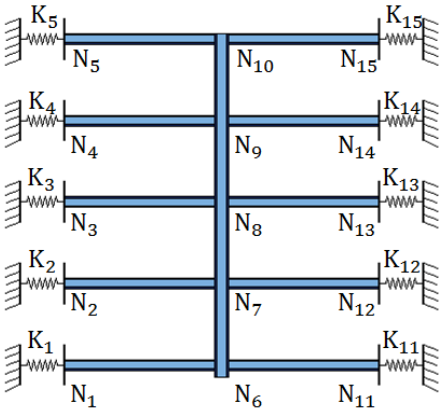

Figure 10. Substructure of the initial damaged part after the loss of column # 26.

K_1	K_2	K_3	K_4	K_5
143,033.2 kN/m	39,917.3 kN/m	19,547.4 kN/m	12,129.2 kN/m	8,143.5 kN/m
K_{11}	K_{12}	K_{13}	K_{14}	K_{15}
143,033.2 kN/m	39,917.3 kN/m	19,547.4 kN/m	12,129.2 kN/m	8,143.5 kN/m

Table 1. Stiffness of springs at each extremity of the substructure after the loss of column # 26.

The non-linear analysis of the substructure corresponding to the initial damaged part (Figure 10) indicates that it achieves to support the applied loads after a certain deflection, where Figure 11 presents the deflection δ_{N_6} at Joint N_6 and the load (Q) diagram, which shows the increment of the substructure capacity due to the development of the tensile membrane action. The substructure achieves to find an alternative equilibrium state under $W_a = 31.6\,KN/m$ with $\delta_{N_6} = 0.63m$.

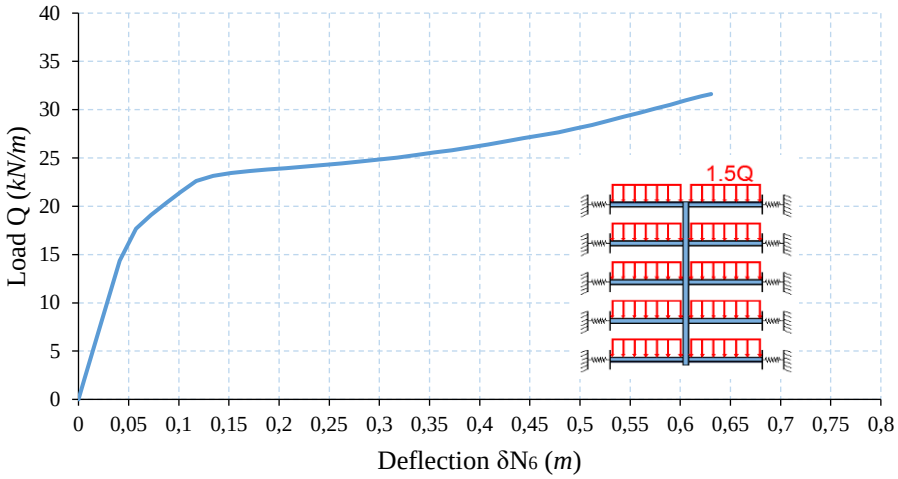

Figure 11. Deflection-load diagram of non-linear static analysis of the initial damaged part after the loss of column # 26.

The tensile membrane action is revealed by the normal force and bending moment diagrams at the joints. Figure 12 shows the effect of large deflections at the joint N_1, where after the bending resistance limit is reached, there is an increase of tensile stress in beams and decrease of bending moment, which helps the structure to reach an alternative equilibrium configuration.

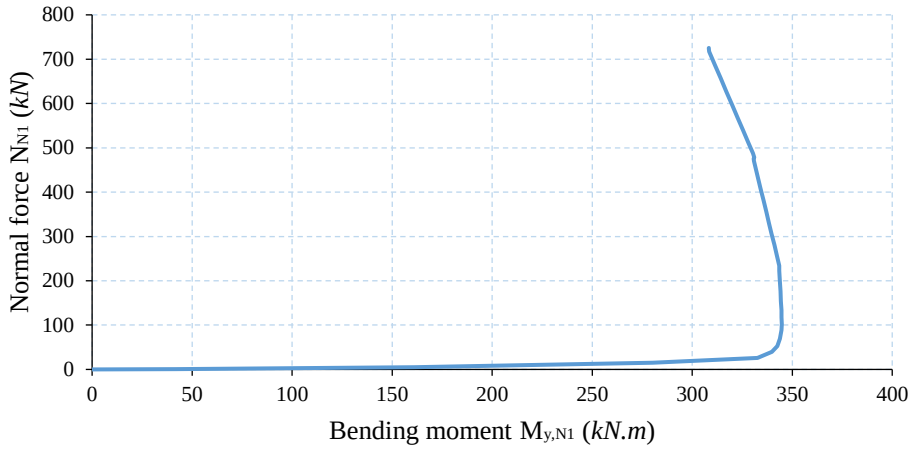

Figure 12 Normal force – Bending moment curve at the joint N_1 after the loss of column # 26.

The non-linear analysis identifies if the substructure can develop an alternating functioning state, and it identifies the geometrical changes that correspond to the new equilibrium state. However, the development of a second line of defence in the substructure does not mean that the indirectly affected part of the structure can resist the horizontal forces developed at the joints. Here, the second iteration of the yield design calculation allows to check if the structure can resist these forces. The geometrical deformation of the substructure identified in the non-linear analysis is integrated in the model for the next iteration of yield calculation, as shown in Figure 13.

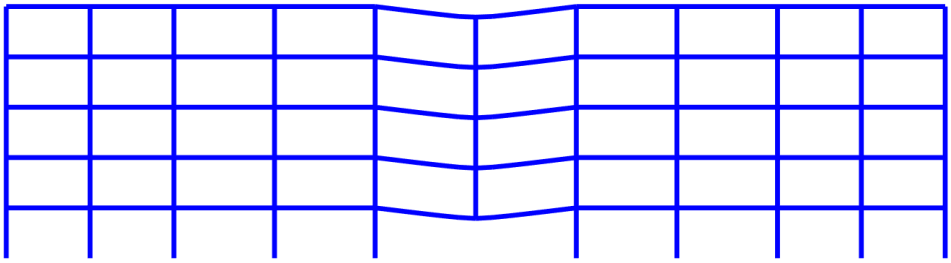

Figure 13. Deformed model of the structure for the second iteration of yield design calculation after the loss of column # 26.

The ultimate loads found in the second iteration of the yield design calculation are $Q_{u,s}^{C2,2} = 32.7\,kN/m$ and $Q_{u,k}^{C2,2} = 33.1\,kN/m$. As $W_a(31.6\,kN/m) < Q_{u,s}^{C2,2}$, the failure of the structure stops in this stage, where there is no other collapse of structural elements and the structure

manages to develop an alternative functioning to resist the propagation of the applied local failure scenario (category C2).

In order to evaluate the assumption to calculate the deformation of the damaged structure by isolating the affected part with considering horizontal springs at the extremities of the substructure, a non-linear static analysis is also performed on the whole structure to identify the margin of error. Figure 14 shows that the maximum vertical deflection of the joint on the top of the removed column $\delta_{26} = 0.67m$. As $\delta_{26}(0.67m) > \delta_{N_6}(0.63m)$, the deflection identified in the analysis of the whole structure is larger than that of the substructure with a relative error about 6%. It is worth to note that the stiffnesses of the horizontal springs at the extremities of the substructure are calculated by a simplified method to represent the response of the indirectly affected part. The rotations of the supports in the substructure are omitted, which may contribute to the difference in the obtained deflection.

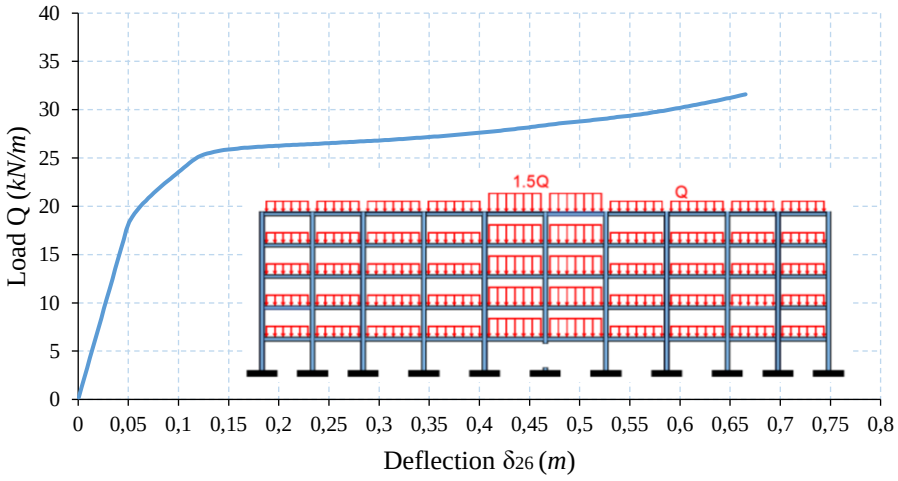

Figure 14. Deflection-load diagram of non-linear static analysis on the whole structure after the loss of column # 26.

Two iterations of yield design calculation and one intermediate non-linear analysis have been done using the proposed coupling strategy with a total computation time $t_{26}^{CS} = 697.0s$, while the non-linear analysis on the whole structure requires $t_{26}^{NL} = 8{,}620.0s$. Hence, for this example one decreases computation cost by 91.9 %.

5.3. Illustration of local failure scenario C3

The third scenario is the notional loss of the columns # 1 and 6 (Figure 15). The ultimate loads of the static and kinematic approaches of the first iteration of the yield design calculation are $Q_{u,s}^{C3,1} = 11.9\,kN/m$ and $Q_{u,k}^{C3,1} = 12.5\,kN/m$. As $Q_{u,s}^{C3,1} < W_a(31.6\,kN/m)$, the structure cannot resist the gravity loads, where the failure mechanism presented in Figure 16 occurs when the bending moment reaches the bending resistance limit of the beams.

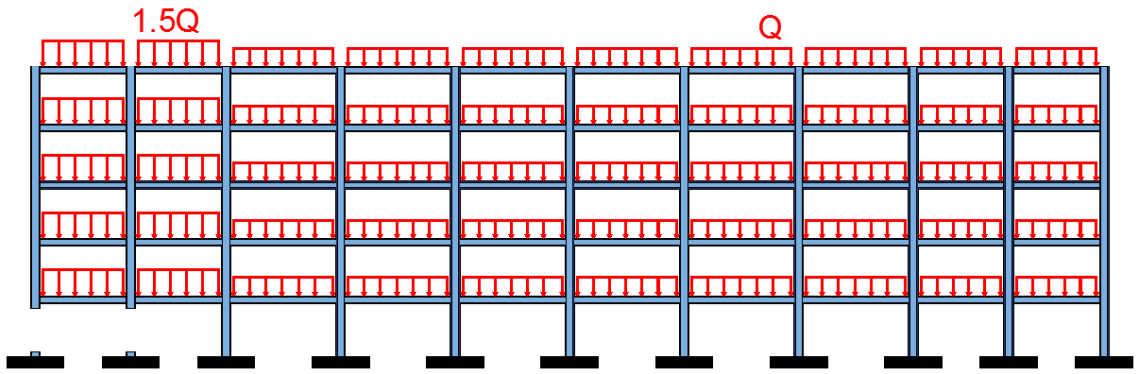

Figure 15. Notional loss of columns # 1 and 6.

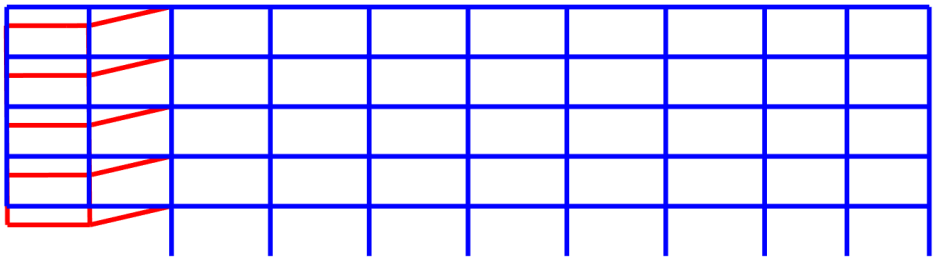

Figure 16. Failure mechanism identified by to first iteration of the yield design calculation after the loss of columns # 1 and 6 (the displacement are not representative).

Furthermore, the failure mechanism identified in Figure 16 indicates the loss of stability of the directly affected part, where there is no possibility of an alternative functioning. Therefore, the affected part is identified automatically by the displacement vector calculated by the kinematic approach of yield design, and it is removed for the next iteration of the yield design calculation (Figure 17). Then, the next iteration indicates that the ultimate loads with the new structural configuration are $Q_{u,s}^{C3,2} = 152\,kN/m$ and $Q_{u,k}^{C3,2} = 159.2\,kN/m$. Hence, $W_a = 31.6\,kN/m < Q_{u,s}^{C3,2}$, and the propagation of the failure stops at this stage with a collapsed part (sum of beams

length) equal to $50m$, which is equal to the initial affected part. Therefore, this scenario corresponds to the category C3 of scenarios for which one observes a collapse of the directly affected part.

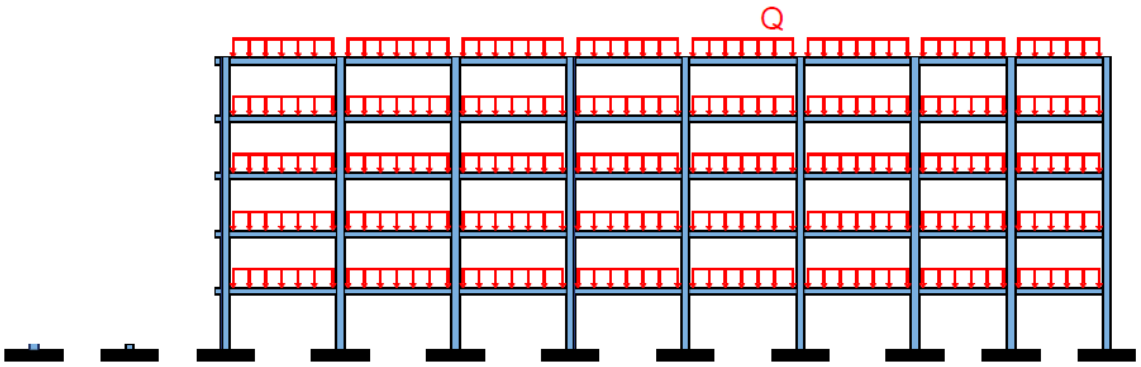

Figure 17. Layout of the structure for the second iteration of the yield design calculation after the loss of columns # 1 and 6.

As a comparison, a non-linear static analysis is applied on the whole structure. Figure 18 shows the maximum vertical deflection δ_1 on the top of the removed column # 1 according to the uniform load Q. As no alternative function can be developed, the load capacity of the structure cannot ensure equilibrium and its maximum value is reached for $\delta_1 > 0.13m$. Hence, the ultimate load is $Q_{u,NL}^{C3} = 12\,kN/m$, where $Q_{u,s}^{C3,1} < Q_{u,NL}^{C3} < Q_{u,k}^{C3,1}$.

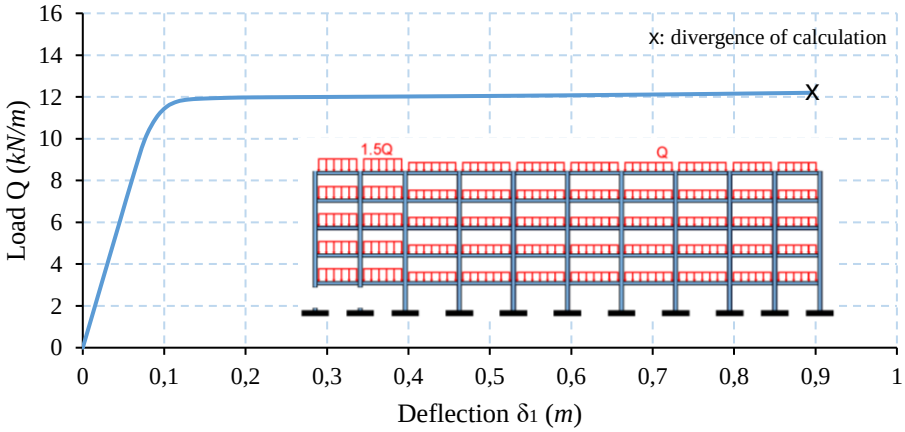

Figure 18. Deflection δ_1-load diagram of non-linear static analysis on the whole structure after the loss of columns # 1 and 6.

When comparing the computation cost of the proposed coupling strategy with the one based on a non-linear analysis of the whole structure, two iterations of yield design calculation are

performed when using the proposed strategy with computation time $t_{C3}^{CS} = 22s$, while the non-linear analysis on the whole structure requires $t_{C3}^{NL} = 1{,}157.0s$.

5.4. Illustration of local failure scenario C4

The fourth scenario is the notional loss of the columns # 11 and 16 (Figure 19). The first iteration of the yield design calculation indicates that $Q_{u,s}^{C4,1} = 14.2\,kN/m$ and $Q_{u,k}^{C4,1} = 15\,kN/m$. As $Q_{u,s}^{C4,1} < W_a = 31.6\,kN/m$, the failure propagates according to the failure mechanism presented in Figure 20.

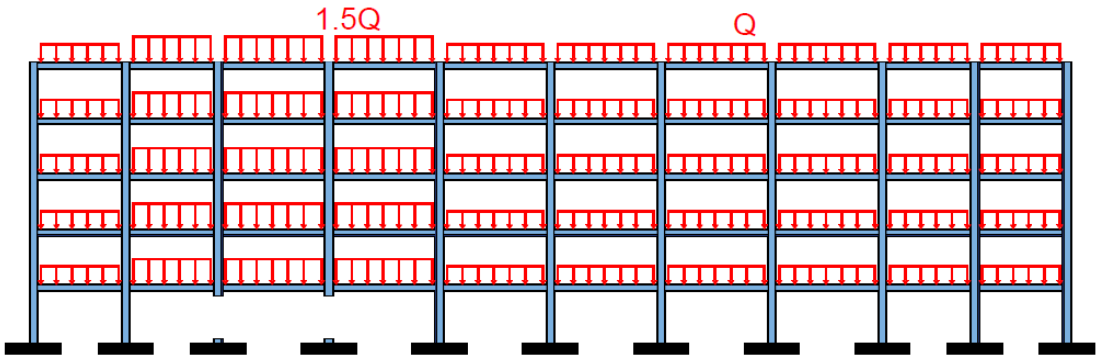

Figure 19. Notional loss of columns # 11 and 16.

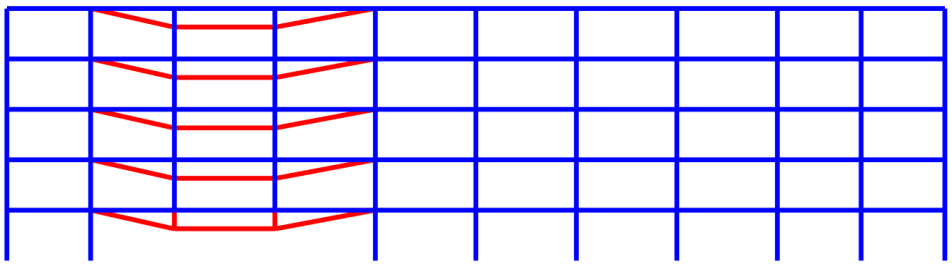

Figure 20. Failure mechanism identified by the first iteration of the yield design calculation after the loss of columns # 11 and 16.

The failure mechanism (Figure 20) indicates that there is a possibility of developing an alternative functioning by the tensile membrane action due to the continuity of the beams on both sides of the affected part. Therefore, a non-linear analysis is performed on the substructure of the affected part (Figure 21). The stiffness of each spring is presented in Table 2.

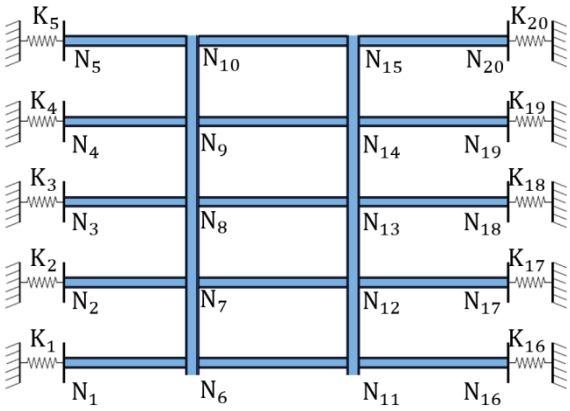

Figure 21. Substructure of the initial damaged part after the loss of columns # 11 and 16.

K_1	K_2	K_3	K_4	K_5
76,726.0 kN/m	15,401.3 kN/m	6,673.7 kN/m	3,852.4 kN/m	2,478.0 kN/m
K_{16}	K_{17}	K_{18}	K_{19}	K_{20}
159,317.8 kN/m	50,690.2 kN/m	26,347.9 kN/m	16,781.2 kN/m	11,277.4 kN/m

Table 2. Stiffness of springs at each extremity of the substructure after the loss of columns # 11 and 16.

Figure 22 presents the diagram of the deflection δ_{N11} on the top of the removed column # 11 and the applied load Q. The load capacity of the structure increases until one reaches the applied load ($W_a = 31.6\,kN/m$), when $\delta_{N11} = 1.13m$. The normal force and bending moment diagram at the joint N_1 (Figure 23) shows the development of the tensile membrane action on the first floor, where the bending moment significantly decreases after the bending resistance limit ($M_{pl}^{IPE360} = 346.0kN.m$) is reached, and the tension force simultaneously increases until $2{,}179.0kN$.

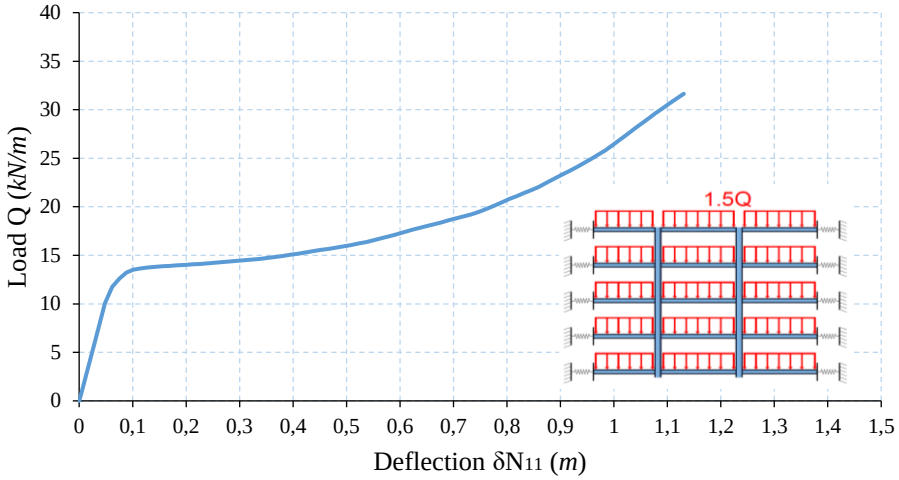

Figure 22. Deflection-load diagram of non-linear static analysis of the initial damaged part after the loss of columns # 11 and 16.

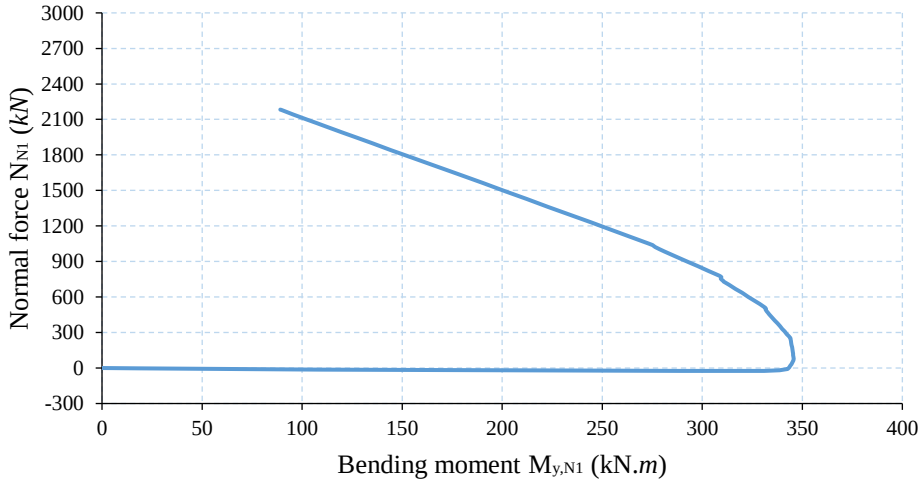

Figure 23. Normal force – Bending moment curve at the joint N_1 after the loss of columns # 11 and 16.

The second iteration of yield design calculation indicates that $Q_{u,s}^{C4,2} = 21.3\,kN/m$ and $Q_{u,k}^{C4,2} = 22.4\,kN/m$. After the large displacement, the ultimate loads of the structure increase compared to the first iteration ($Q_{u,s}^{C4,2} > Q_{u,s}^{C4,1}$ and $Q_{u,k}^{C4,2} > Q_{u,k}^{C4,1}$), while $Q_{u,s}^{C4,2} < W_a = 31.6\,kN/m$. Hence, the indirectly affected part of the structure is not able to resist the forces developed during the development of the tensile membrane action. Figure 24 shows the failure mechanism, which reveals that the part on the left side of the initial affected part cannot support the forces developed after the geometrical deformation. The normal forces that developed in the initial affected part lead to an increment in the bending moment at the bottom of columns in the

indirectly affected part, as shown in Figure 25, where the bending moment at b1 and b2 reaches the bending limit of the column element.

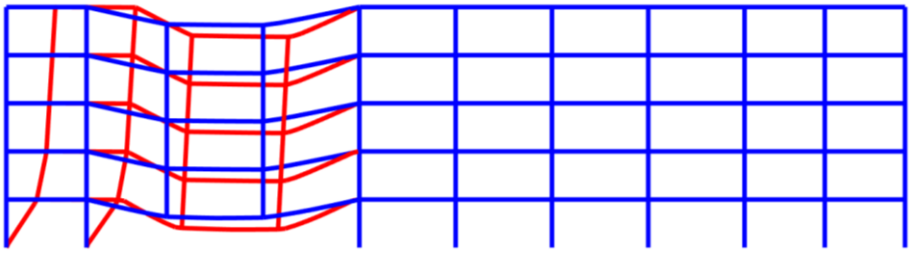

Figure 24. Failure mechanism identified by the second iteration of the yield design calculation after the loss of columns # 11 and 16.

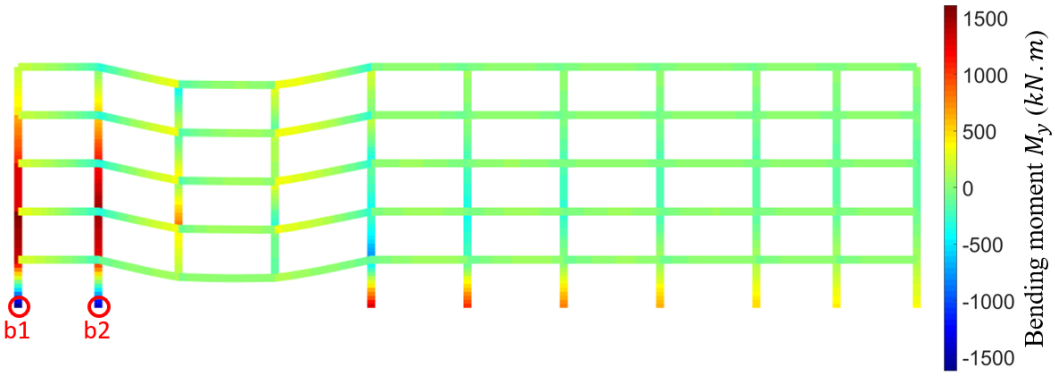

Figure 25. Bending moment diagram according to the second iteration of the yield design calculation after the loss of columns # 11 and 16 ($M_{y0}^{IPE360} = 346.0kN.m$ and $M_{y0}^{HE500B} = 1{,}662.0kN$).

The failure mechanism indicates the loss of stability of the affected part, where it is removed for the next iteration of the yield design calculation, as shown in Figure 26. Finally, the ultimate loads identified are $Q_{u,s}^{C4,3} = 152\,kN/m$ and $Q_{u,k}^{C4,3} = 159.2\,kN/m$, which means that the collapse stops at this stage as $W_a = 31.6\,kN/m < Q_{u,s}^{C4,3}$. The beam total lengths of the initially affected and the collapsed parts for this scenario are equal to $85m$ and $110m$, respectively. Therefore, the collapse expands out of the directly affected part and this scenario falls in category C4.

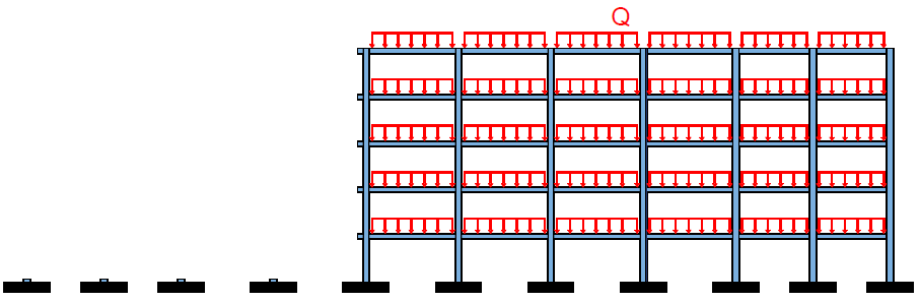

Figure 26. Layout of the structure for the third iteration of the yield design calculation after the loss of columns # 11 and 16.

Similarly to the previous illustrative examples in categories C1, C2, and C3, a non-linear static analysis is applied on the whole structure for comparison with the coupling approach. The divergence of calculation occurs when the deflection $\delta_{16} = 1.46m$ on the top of removed column # 16 (Figure 27), where the load capacity of the structure increases until $Q_{u,NL}^{C4} = 25.4\,kN/m$. Plastic hinges are developed at the base supports b1 and b2, as shown in Figure 28, which indicates the development of a failure mechanism on the indirectly affected part. The bending moment at b2 is lower than that of b1 due to the high compression force developed in the column # 6 (Figure 29), while a tension force is developed in the column # 1, where the rotation of the indirectly affected on the left side leads to this aspect.

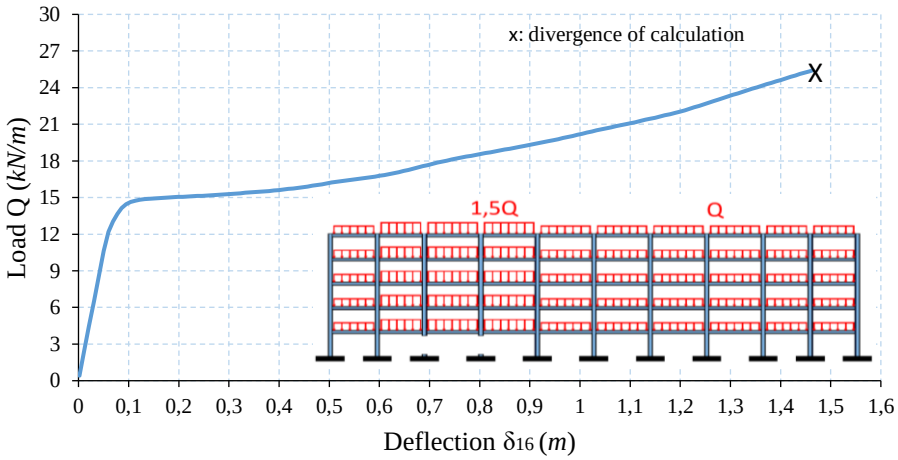

Figure 27. Deflection δ_{11}-load diagram of non-linear static analysis on the whole structure after the loss of columns # 11 and 16.

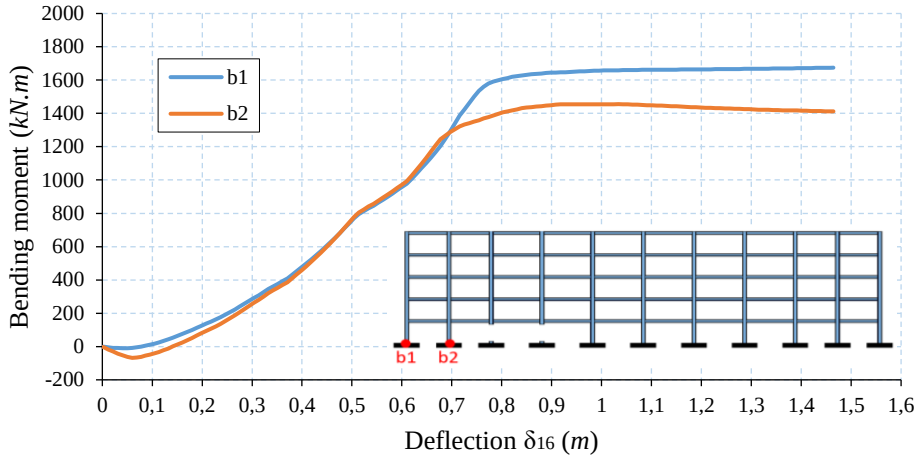

Figure 28. Deflection δ_{16}-bending moment diagram at base supports after the loss of columns # 11 and 16.

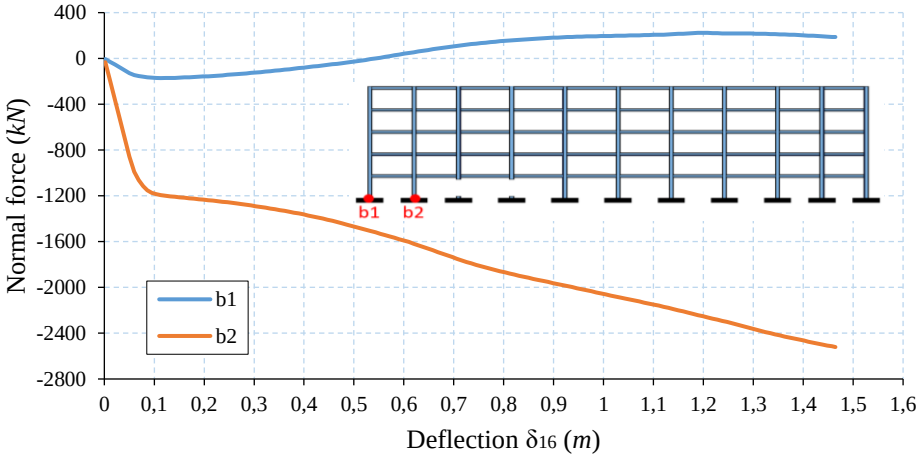

Figure 29. Deflection δ_{16}- normal force diagram at base supports after the loss of columns # 11 and 16.

The computation time of the non-linear analysis on the whole structure is $t_{C4}^{NL} = 12{,}351.0s$. The use of the proposed coupling strategy indicates that three iterations of yield design calculation and one iteration of non-linear analysis on the substructure of the directly affected part are performed, where the total computation cost is $t_{C4}^{CS} = 1{,}105.0s$.

6. CONCLUSIONS

An original structural modelling strategy is proposed and based on an iterative coupling between the yield design approach and a non-linear analysis, to simulate progressive collapse. The adoption of the yield design theory allows a simplification in the analysis of the structural response. It is a direct approach that significantly saves computation time and mitigates

convergence issues. One main drawback of yield design theory is that one does not identify the capacity of the structure to find a new behaviour (catenary action) under large displacements as this behaviour is not investigated by this theory. A non-linear analysis based on a corotational formulation is then used to analyze the structural response of the part concerned by the failure mechanism. One can analyze the development of an alternative functioning in the directly affected part, and simulate the geometrical and the material non-linearities. The successive iterations of the yield design approach with the deformed geometrical configuration allow to check the ability of the structure to develop a second line of defence.

The illustrative example shows the capacity of the proposed coupling strategy to model the failure propagation by identifying the initial and the final states of collapse. Besides, the comparison of the computation time shows the capacity of this strategy to decrease this time compared to a full non-linear analysis on the whole structure. One can investigate in a reasonable computation time a large number of local failure scenarios, so a general assessment of structural robustness can be performed.

It should be noted that several assumptions were made for simplification and that further work should be considered before considering the illustrative example for wider applications. Indeed, the affected part was isolated each time for non-linear analysis with a simplified modelling of the joints at the edges. As the objective of this work was not to develop a macro-model of connections but rather to focus on a strategy to iteratively follow the failure propagation, this assumption was adopted herein. Some further development are obviously required as the omission of the rotations of the supports in the sub-structure can cause an error in the prediction of the deflection. Joint behaviour strongly influences progressive collapse (strength, stiffness and deformation capacity) and an accurate modelling is needed to cater for important features of real behaviour. Also, including the displacement of the indirectly affected part should be considered to properly take into account P-delta effects. For the risk of buckling, the Euler load

formulation was used as a first approximation and an adequate interaction relationship between axial compression and bending should be used in future studies for beam-column elements. Several research works in the literature have already developed macromodels for modelling in an accurate way the response of supports in submodels (Bao et al., 2008; Sadek et al., 2008; Vlassis et al., 2008; Vidalis, 2014) and integration of these developments in the proposed framework represents an interesting perspective. Also, the comparison with other approaches for numerical modelling should be considered (Li et al. 2018; Zhang et al. 2020). Some analytical methods (Demonceau, 2008; Huvelle et al., 2015) are proposed in the literature to predict the response of a frame structure submitted to a column loss with isolating the directly affected part. As these methods enable to identify the geometrical deformation under the applied loads, they can replace the iteration of the non-linear analysis in the proposed iterative strategy, which could again reduce the computation cost.

The methodology was applied to steel framed structures. An application to other materials such as reinforced concrete elements should be considered to investigate the potential of coupling between the yield design theory and non-linear analyses. Future research is needed to test other non-linear finite element models (with different formulations, Lagrangian, updated Lagrangian and corotational) and/or adapt the iterative coupling strategy for different types of materials. The comparison with previous studies, both numerical and experimental, should be considered for the implementation of the proposed approach and reinforced concrete structures (Parisi and Scalvenzi, 2020, Kiakojouri et al. 2020, Yu et al. 2020, Qiang et al. 2020).

This work aims to be used in the future, by providing some recommendations on design for robustness, in link with the evolution of standards (revision of Eurocodes related to robustness, development of technical recommendations for robustness for fib Model Code 2020).

REFERENCES

Adam, J.M., Parisi, F., Sagaseta, J., Lu, X. 2018. Research and practice on progressive collapse and robustness of building structures in the 21st century. *Engineering Structures* 173, 122–149.

Baker, J.F., Williams, E.L., Lax, D. 1948. The design of framed buildings against high explosive bombs, in: The Civil Engineer in War: Properties of Materials, Structures, Hydraulics, *Tunnelling and Surveying*. pp. 80–112.

Baker, J.W., Schubert, M., Faber, M.H. 2008. On the assessment of robustness. *Structural Safety* 30, 253–267.

Bao, Y., Kunnath, S.K., El-Tawil, S., Lew, H.S. 2008. Macromodel-Based Simulation of Progressive Collapse: RC Frame Structures. *Journal of Structural Engineering* 134, 1079–1091.

Bao, Y., Main, J.A., Lew, H.S., Sadek, F. 2014. Robustness Assessment of RC Frame Buildings under Column Loss Scenarios, in: Structures Congress 2014. Presented at the Structures Congress 2014, American Society of Civil Engineers, Boston, Massachusetts, United States, pp. 988–1001.

Bleyer, J. 2015. Méthodes numériques pour le calcul à la rupture des structures de génie civil. Paris-Est University, Doctoral School of Sciences, Ingénierie et Environnement.

Bleyer, J., de Buhan, P. 2013. Yield surface approximation for lower and upper bound yield design of 3D composite frame structures. *Computers & Structures* 129, 86–98.

COST Action TU0601, 2011. Robustness of Structures - theoretical framework on structural robustness.

DCLG, CPNI, 2011. Review of international research on structural robustness and disproportionate collapse. Department for Communities and Local Government, and Centre for the Protection of National Infrastructure, London.

De Buhan, P., 2007a. Plasticité et calcul à la rupture.

De Buhan, P., 2007b. Plasticité et calcul à la rupture.

Demonceau, J.-F. 2008. Steel and composite building frames: sway response under conventional loading and development of membrane effects in beams further to an exceptional action. University of Liege.

Demonceau, J.-F., D'Antimo, M., Jaspart, J.-P. 2018. Robustness of steel structures subjected to a column loss scenario. Presented at the 6th International Symposium on Life-Cycle Civil Engineering, Ghent, Belgium.

Droogné, D., Botte, W., Caspeele, R. 2018. A multilevel calculation scheme for risk-based robustness quantification of reinforced concrete frames. Engineering Structures 160, 56–70.

El Hajj Diab, M., Orcesi, A., Desprez, C., Bleyer, J. 2019. An embedded yield design approach within anon-linear analysis for structural modeling of progressive collapse. Presented at the RILEM spring convention and sustainable materials, systems and structures conference, Rovinj, Croatia.

El Hajj Diab, M. 2019. Analysis of structural robustness - Characterization of accidental/exceptional actions and their impacts on structures, PhD thesis, Université Paris-Est.

El Kamari, Y., Raphael, W., Chateauneuf, A. 2015. Reliability study and simulation of the progressive collapse of Roissy Charles de Gaulle Airport. Case Studies in Engineering Failure Analysis 3, 88–95.

EN 1990, 2003. EN 1990: Eurocode - basis of structural design.

Faber, M.H., Maes, M.A., Straub, D., Baker, J. 2006. On the Quantification of Robustness of Structures, OMAE2006, 25th International Conference on Offshore Mechanics and Arctic Engineering, Hamburg, Germany, June 4-9.

fib, 2012. Model Code 2010 - Final draft, Volume 2.

Filippou, F.C., Constantinides, M. 2004. FEDEASLab getting started guide and simulation examples. Technical report NEESgrid-TR22.

Fu, F. 2010. 3-D nonlinear dynamic progressive collapse analysis of multi-storey steel composite frame buildings — Parametric study. *Engineering Structures* 32, 3974–3980.

Gao, S., Guo, L., Fu, F., Zhang, S. 2017. Capacity of semi-rigid composite joints in accommodating column loss. *Journal of Constructional Steel Research* 139, 288–301.

GSA, 2003. Progressive Collapse Analysis and Design Guidelines for New Federal Office Buildings and Major Modernization Projects. Washington, DC: Office of Chief Architects.

Hoffmann, N., Kuhlmann, U., Demonceau, J.-F., Jaspart, J.-P., Colomer, C., Hoffmeister, B., Zandonini, R., Hjiaj, M., Mohler, C. 2015. Robust Impact Design of Steel and Composite Buildings. IABSE Symposium Report 103, 38–45.

Huvelle, C., Hoang, V.-L., Jaspart, J.-P., Demonceau, J.-F. 2015. Complete analytical procedure to assess the response of a frame submitted to a column loss. *Engineering Structures* 86, 33–42.

Izzuddin, B.A., Vlassis, A.G., Elghazouli, A.Y., Nethercot, D.A. 2008. Progressive collapse of multi-storey buildings due to sudden column loss — Part I: Simplified assessment framework. *Engineering Structures* 30, 1308–1318.

Jaspart, J.P., Demonceau, J.F., Ludivine, C. 2011. Robustness of steel and composite building structures. Presented at the 7th National conference on steel structures, Grèce Volos.

Kagho-Gouadjio, N.C., Orcesi, A.D. Cremona, C. & Marcotte, C. 2015. Quantification of structural robustness: application to the study of a prestressed concrete beam, *Mechanics & Industry*, 16(1), 104.

Kazemi-Moghaddam, A., Sasani, M. 2015. Progressive collapse evaluation of Murrah Federal Building following sudden loss of column G20. *Engineering Structures* 89, 162–171.

Kiakojouri, F., De Biagi, V., Chiaia, B. & Reza Sheidaii, M. (2020). Progressive collapse of framed building structures: Current knowledge and future prospects. *Engineering Structures*, 206.

Le, T.N. 2013. Nonlinear dynamics of lexible structures using corotational beam elements. INSA Rennes.

Le, T.-N., Battini, J.-M., Hjiaj, M. 2014. Corotational formulation for nonlinear dynamics of beams with arbitrary thin-walled open cross-sections. Computers & Structures 134, 112–127.

Le, T.-N., Battini, J.-M., Hjiaj, M. 2011. Efficient formulation for dynamics of corotational 2D beams. Comput Mech 48, 153–161.

Li, L.-L., Li, G.-Q., Jiang, B. & Lu, Y. (2018). Analysis of robustness of steel frames against progressive collapse. *Journal of Constructional Steel Research*. 143, 264-278.

Li, Y., Lu, X., Guan, H., Ren, P., Qian, L. 2016. Probability-based progressive collapse-resistant assessment for reinforced concrete frame structures. *Advances in Structural Engineering* 19, 1723–1735.

Li, Y., Lu, X., Guan, H., Ye, L. 2011. An improved tie force method for progressive collapse resistance design of reinforced concrete frame structures. *Engineering Structures* 33, 2931–2942.

Lu, X., Li, Y., Guan, H., Ying, M. 2017. Progressive Collapse Analysis of a Typical Super-Tall Reinforced Concrete Frame-Core Tube Building Exposed to Extreme Fires. *Fire Technology* 53, 107–133.

Marchand, K.A., Alfawakhiri, F. 2005. Facts for Steel Buildings-Blast and Progressive Collapse.

Marginean, I., Dinu, F., Dubina, D. 2018. Simulation of the dynamic response of steel moment frames following sudden column loss. Experimental calibration of the numerical model and application. *Steel Construction* 11, 57–64.

Mazars, J., Grange, S. 2017. Simplified strategies based on damage mechanics for concrete under dynamic loading. Philosophical Transactions of the Royal Society A: Mathematical, Physical and Engineering Sciences 375, 20160170.

Mosek, A. P. S. 2010. The MOSEK optimization software. *Online at http://www. mosek. com*, *54*(2-1), 5.

Nafday, A.M. 2011. Consequence-based structural design approach for black swan events. *Structural Safety*, 33, 108–114.

Neuenhofer, A., Filippou, F.C., 1997. Evaluation of Nonlinear Frame Finite-Element Models. *J. Struct. Eng*. 123, 958–966. https://doi.org/10.1061/(ASCE)0733-9445(1997)123:7(958)

Nutal, B. 2014. Robustness of Steel and Concrete Structures. Université de Liège.

NF EN 1990, 2003. Basis of structural design. Comité européen de Normalisation (CEN).

NF EN 1991-1-1, 2003. Eurocode 1, Actions on structures, Part 1-1: General actions — Densities, self weight, imposed loads for buildings.

NF EN 1992-1-1, 2005. Design of concrete structures.

NIST, 2006. Final Report on the Collapse of the World Trade Centre Towers. National Institute of Standards and Technology, Gaithersburg, MD.

NTSB, 2008. Collapse of I-35W Highway Bridge Minneapolis, Minnesota August 1, 2007.

Parisi, F. & Scalvenzi, M. (2020). Progressive collapse assessment of gravity-load designed European RC buildings under multi-column loss scenarios. *Engineering Structures*, 209.

Pearson, C., Delatte, N. 2005. Ronan Point Apartment Tower Collapse and its Effect on Building Codes. *Journal of Performance of Constructed Facilities* 19, 172–177.

Pham, D.T. 2014. Analyse par le calcul à la rupture de la stabilité au feu des panneaux en béton armé de grandes dimensions. Paris-Est University.

Qiang, H., Yang, J., Feng, P. & Qin, W. (2020). Kinked rebar configurations for improving the progressive collapse behaviours of RC frames under middle column removal scenarios. *Engineering Structures*, 211.

Sadek, F., El-Tawil, S., Lew, H.S. 2008. Robustness of Composite Floor Systems with Shear Connections: Modeling, Simulation, and Evaluation. *Journal of Structural Engineering* 134, 1717–1725.

Sadek, F., Main, J.A., Lew, H.S., Bao, Y. 2011. Testing and Analysis of Steel and Concrete Beam-Column Assemblies under a Column Removal Scenario. *Journal of Structural Engineering* 137, 881–892.

Salençon, J. 2013. Yield design, Mechanical engineering and solid mechanics series. ISTE ; Wiley, London : Hoboken, NJ.

Sasani, M. 2008. Response of a reinforced concrete infilled-frame structure to removal of two adjacent columns. *Engineering Structures* 30, 2478–2491.

Song, B.I., Sezen, H. 2013. Experimental and analytical progressive collapse assessment of a steel frame building. *Engineering Structures* 56, 664–672.

Salençon, J. 2013. *Yield design*. John Wiley & Sons.

Spacone, E., Filippou, F.C., Taucer, F.F. 1996. Fibre beam-column model for non-linear analysis of r/c frames: part I. Formulation. *Earthquake Engineering & Structural Dynamics* 25, 711–725.

Stylianidis, P. 2011. Progressive collapse response of steel and composite buildings. Department of Civil and Environmental Engineering-Imperial College London.

Sun, R., Huang, Z., Burgess, I.W. 2012. Progressive collapse analysis of steel structures under fire conditions. *Engineering Structures* 34, 400–413.

Tagel-Din, H., Meguro, K. 2000. Applied element method for simulation of nonlinear materials: theory and application for RC structures. *Structural Eng. Earthquake Eng.*, International Journal of the Japan Society of Civil Engineers (JSCE) 17, 137–148.

UFC 4-023-03, 2009. Design of buildings to resist progressive collapse.

Ulm, F-J . 1996. Un modèle d'endommagement plastique: application aux bétons de structure. Laboratoire central des ponts et chaussées.

Vidalis, C.A. 2014. Improving the resistance to progressive collapse of steel and composite frames. Imperial College London-Department of Civil and Environmental Engineering.

Vincent, H., Arquier, M., Bleyer, J., de Buhan, P. 2017. Yield design based numerical analysis of three-dimensional reinforced concrete structures. 4th International conference on Mechanical Models in Structural Engineering, Dec. 2017, Madrid, Spain.

Vlassis, A.G., Izzuddin, B.A., Elghazouli, A.Y., Nethercot, D.A. 2008. Progressive collapse of multi-storey buildings due to sudden column loss—Part II: Application. *Engineering Structures* 30, 1424–1438.

Yu, J., Tang, J.-H., Luo, L.-Z. & Fang, Q. (2020). Effect of boundary conditions on progressive collapse resistance of RC beam-slab assemblies under edge column removal scenario. *Engineering Structures*, 225.

Zhang, J.Z., Jiang, B.-H., Feng, R. & Chen, R. (2020). Robustness of steel moment frames in multi-column-removal scenarios. *Journal of Constructional Steel Research*, 175.

Zhao, X.-L., Wilkinson, T., Hancock, G. 2005. Members Subjected to Bending and Compression, in: *Cold-Formed Tubular Members and Connections*. Elsevier, pp. 91-116.